Iterative Frequency Domain Joint-over-Antenna Detection in Multiuser MIMO

Juha Karjalainen, *Student Member, IEEE,* Nenad Veselinović, *Member, IEEE,* Kimmo Kansanen, *Member, IEEE*, and Tad Matsumoto, *Senior Member, IEEE*

***Abstract*— Multiuser multiple-input-multiple-output (MIMO) wireless systems have great potential in improving information rate, diversity and resistance to against interference. The primary objective of this paper is to derive for broadband signaling a new iterative frequency domain (FD) multiuser MIMO signal detection technique for joint-over-antenna (JA) detection. The proposed detector is based on soft-cancellation and minimum mean square error (MMSE) filtering, followed by maximum a posteriori probability (MAP) detector to detect several of each users transmit antennas. The purpose of jointly detecting several transmit antennas is to preserve the degrees of freedom (DoF) for MMSE. Computational complexities with FD and its time domain (TD) counterpart are evaluated in this paper, and it is shown that FD requires significantly lower complexity than TD. Numerical results show that JA significantly outperforms the receiver that detects transmit antenna signals antenna-by-antenna (AA). The proposed iterative FD JA technique achieves larger performance gains compared to AA when the total number of transmit antennas is larger than the number of receiver antennas, as well as in the presence of spatial correlation.**

***Index Terms*— Multiuser MIMO, spatial multiplexing, turbo coding, iterative processing, frequency domain equalization.**

I. Introduction

MULTIUSER multiple-input-multiple-output (MIMO) systems have been recognized for future wireless broadband communications as being one of the most powerful and flexible radio network configurations that have great potential in improving drastically the information rate, diversity, and resistance against interference. A major challenge in uplink communications of broadband multiuser MIMO systems is to create a receiver algorithm that can efficiently and effectively detect the multiple signals, transmitted from multiple antennas of multiple users.

Since the discovery of turbo codes in 1993 [1], iterative processing, called the turbo principle, has been applied to solving the complexity problems of optimal joint equalization and decoding [2],[3],[4],[5], and multiuser detection for coded communication systems [6],[7]. Because of its exponentially increasing complexity, the optimal maximum *a* posteriori probability (MAP)-based multiuser iterative detector is practical only for small numbers of users and of transmit antennas as well as in short delay spread channels with relatively simple modulation formats, like binary (BPSK) and quadrature phase shift keying (QPSK). Therefore, it has been of great importance to reduce the computational complexity of iterative receivers for practical applications in future broadband systems where large number of users, each having multiple transmit antennas and using high order modulation formats, are expected to be located in the cells.

In future broadband wireless systems it is expected that high data rate services are demanded also in uplink communications. The fact that the transmission power of portable wireless terminal is limited due to the battery longevity and large propagation loss due to broadband transmission over multipath mobile communication channels at a higher centre carrier frequency requires breakthrough-techniques, if a relatively large per-cell coverage is aimed at: Obviously, it is desirable to use a radio signalling scheme that does not require large power consumption for transmission. In [8],[9] it is stated that orthogonal frequency-division multiplexing (OFDM) requires a relatively larger peak-to-average power ratio (PAPR) than single carrier signalling: OFDM requires a larger power back-off, resulting in a larger power consumption than single carrier signalling. Therefore, recently, practical comparison of those signalling techniques for uplink has been a core discussion topic of the research community. Although several techniques have been known that can effectively reduce OFDMs relatively large PAR [10], it is out of the scope of this paper.

Broadband single carrier multiuser MIMO communications require receivers to be able to reduce the distortions caused by co-channel-interference (CCI) and inter-symbol interference (ISI). One of the most promising low complexity techniques that can achieve excellent performance without requiring prohibitively high computational complexity is the iterative soft-cancellation (SC) and minimum mean square error (MMSE) filtering-based receiver (SC-MMSE) [6] and its family [11],[4]. The computational complexity of original SC-MMSE is approximately of a cubic order of the length, RL, for time-domain MMSE filtering where R is the number of receiver antennas and L is the length of the channel.

The techniques proposed in [6] and [11] aim to detect

Manuscript received February 23, 2006; revised November 14, 2006; accepted May 3, 2007. The associate editor coordinating the review of this paper and approving it for publication was R. M. Buehrer. This work was funded in part by the Academy of Finland under grant 112970, A part of this paper was presented at the Thirty-Ninth Asilomar Conference on Signals Systems and Computers, October 30-November 2 2005, Pacific Grove, CA, USA. Another part was presented at Turbo-Coding-2006, 4th International Symposium on Turbo Codes & Related Topics, 3-7 April 2006, Munich, Germany.

J. Karjalainen and T. Matsumoto are with the Centre for Wireless Communications, University of Oulu, FIN-90014, Oulu, Finland (e-mail: {juha.karjalainen, tadashi.matsumoto}@ee.oulu.fi).

N. Veselinović is with Elektrobit Ltd, Finland (e-mail: nenad.veselinovic@elektrobit.com).

K. Kansanen is with the Norwegian Univiversity of Science and Technology (NTNU), Norway (e-mail: kimmo.kansanen@iet.ntnu.no).

Digital Object Identifier 10.1109/TWC.2007.060037.

signals transmitted from the multiple antennas on antenna-by-antenna (AA) basis. In the AA detection the MMSE filter has to suppress residual interference after interference cancellation and separates the users and antennas. Therefore, the available degrees of freedom (DoF) for the MMSE filtering is decreased, depending on the significance of residual interference [12]: It is expected that their performances are degraded in overloaded situations where the number of the transmit antennas is larger than the receiver's. Recently, [12] proposed a joint-over antenna (JA) signal detection technique based on SC-MMSE for multiuser MIMO systems. Reference [12]'s proposed technique extends the idea of non-iterative joint detection of multiuser signals, presented in [13], by combining the idea with iterative SC-MMSE technique. The aim of jointly detecting several transmit antennas is to preserve DoF for MMSE, and thereby JA's performance in overloaded scenario is better than AA's. However, in [12] signal processing for the JA detection is performed in the time domain, and therefore the cubic order complexity is still required.

Since the early 1970s frequency domain equalization has been known as one of the most powerful ISI compensation techniques for single-carrier signalling [14]. Especially, since mid 1990s it has been more focused than before, and combined with cyclic prefix transmission allowing for computationally efficient Fast Fourier Transform (FFT) and its inverse [15] to be used in the receiver. The resulting system is computationally comparable to OFDM due to its block-wise processing [8].

In the last couple of years, the SC-MMSE techniques have been intensively researched in, eg [16], [11],[17], all with the common aim of reducing its computational complexity. Recent advances in iterative frequency domain processing [18],[19],[20],[21] have demonstrated the great potential of iterative frequency-domain processing techniques in providing excellent performances without requiring heavy computational efforts compared to the time domain methods.

So far, the most of the research work in this areas has focused only on point-to-point MIMO communications with AA-based frequency domain iterative receivers. Only, recently [22] proposed an iterative frequency domain JA MIMO receiver for point-to-point communications. The primary objective of this paper is, therefore, to derive a new multiuser MIMO detector based on JA SC-MMSE that achieves robustness and excellent performance in severe multipath channels. To achieve this goal, we shall extend the frequency domain technique presented in so that the extended algorithm works properly in multiuser scenarios without requiring heavy computational efforts. In fact, the algorithm and the results were in part presented in a conference paper [23], however, because of the space limitation, it only outlines the technique: This paper details the algorithm derivation and performance results.

This paper is organizes as follows: In Section 2 the system model considered in this paper is introduced. Section 3 derives the exact and approximated solutions to the optimization problem associated with FD multiuser MIMO SC-MMSE. Section 4 provides the results of computational complexity analysis for the proposed detector. In Section 5 numerical results of frequency domain JA multiuser MIMO receivers are presented. Finally, Section 6 concludes this paper.

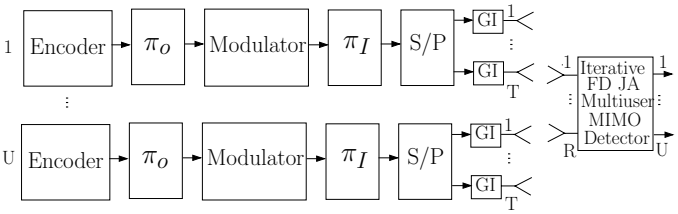

Fig. 1. Vertically coded spatially multiplexed multiuser MIMO system.

II. System Model

This paper considers vertically encoded spatially multiplexed multiuser MIMO system, known as vertical Bell Labs Layered Space-Time transmission (V-BLAST) [24], where receiver has R antennas and there are U users each having T transmit antennas. A model of the considered system is depicted in Fig. 1, where a turbo code is assumed as the vertical code [25]. The encoded sequences are bit-interleaved and modulated symbols are further interleaved at the symbol level. The serial data stream is uniformly demultiplexed to form parallel independent symbol streams, called layers, which are simultaneously transmitted from the T transmit antennas using the same frequency and the same time slots. The system uses cyclic-prefix single carrier burst transmission. Since the cyclic-prefix burst transmission technique is very well known [8], details are not described in this paper. After guard period removal,[1] a space-time presentation of the signal vector $\tilde{\mathbf{r}} \in \mathbb{C}^{RK\times 1}$ received by the R received antennas is given by

$$\mathbf{r} = \hat{\mathbf{H}}\mathbf{b} + \mathbf{v}, \tag{1}$$

where $\mathbf{v} \in \mathbb{C}^{RK\times 1}$ is a white additive independent identically distributed (i.i.d) Gaussian noise vector with variance σ^2 per dimension, with K being the length of discrete fourier transform (DFT), and $\mathbf{b} \in \mathbb{C}^{UTK\times 1}$ is the transmitted multiuser signal vector

$$\mathbf{b} \quad = \quad [\mathbf{b}^1, ..., \mathbf{b}^u, ..., \mathbf{b}^U]^\dagger \tag{2}$$

with $\mathbf{b}^u \in \mathbb{C}^{TK\times 1}$ and $u = 1, ..., U$. The sub-vectors $\mathbf{b}^u$ of $\mathbf{b}$ is given by

$$\mathbf{b}^u \quad = \quad [\mathbf{b}^{u,1}, ..., \mathbf{b}^{u,t}, ..., \mathbf{b}^{u,T}]^\dagger \tag{3}$$

denoting the u^{th} user's transmitted layers over the T transmit antennas. $\mathbf{b}^{u,t} \in \mathbb{C}^{K\times 1}$ is given by

$$\mathbf{b}^{u,t} \quad = \quad [b_1^{u,t}, ..., b_k^{u,t}, ..., b_K^{u,t}]^\dagger, \tag{4}$$

where $t = 1, ..., T$ and $k = 0, ..., K-1$ contain transmitted symbols of the u^{th} user's t^{th} layer. The sum power over all layers per user is normalized to one at every symbol time instant. † indicates vector/matrix transpose operation. The circulant block channel matrix $\hat{\mathbf{H}} \in \mathbb{C}^{RK\times UTK}$ is then given as

$$\hat{\mathbf{H}} \quad = \quad [\hat{\mathbf{H}}_1, ..., \hat{\mathbf{H}}_u, ..., \hat{\mathbf{H}}_U], \tag{5}$$

[1]We restrict ourselves to case where the length of guard period is larger than or as large as the channel memory length.

where $\hat{\mathbf{H}}_u \in \mathbb{C}^{RK\times TK}$ with $u = 1,\cdots,U$ is a circulant block matrix corresponding to the u^{th} user. The circulant block matrix for the u^{th} user is denoted as

$$\hat{\mathbf{H}}_u = \begin{bmatrix} \hat{\mathbf{H}}_u^{1,1} & \dots & \hat{\mathbf{H}}_u^{1,T} \\ \vdots & \ddots & \vdots \\ \hat{\mathbf{H}}_u^{R,1} & \dots & \hat{\mathbf{H}}_u^{R,T} \end{bmatrix}, \tag{6}$$

where the channel submatrices $\hat{\mathbf{H}}_u^{r,t} \in \mathbb{C}^{K\times K}$ between the t^{th} transmit and the r^{th} receive antennas, $r = 1,...,R$, are also circulant, as

$$\hat{\mathbf{H}}_u^{r,t} = circ\left\{\left[h_{u,1}^{r,t}, h_{u,2}^{r,t}\dots h_{u,L}^{r,t}\right]^\dagger\right\}. \tag{7}$$

The operator $circ\{\ \}$ generates matrix that has a circulant structure of the argument of the operator. L denotes the length of the channel, and $h_{u,l}^{r,t}$, $l = 1,...,L$, the fading gains of multipath channel between the u^{th} user's t^{th} transmit antenna and the r^{th} receive antenna. For the each user's transmit-receive antenna pair the sum of the average power of fading gains is normalized to one.

It is well known that the circulant matrices can be diagonalized by the unitary DFT matrix $\mathbf{F} \in \mathbb{C}^{K\times K}$ [26] with the elements $f_{m,k} = \exp\frac{j2\pi mk}{K}$, where $m,k = 0,...,K-1$. Similarly, the circulant block matrices can be block-diagonalized by using block diagonal DFT matrices. The block-diagonalization of $\hat{\mathbf{H}}$ is performed as

$$\hat{\mathbf{H}} = \mathbf{F}_R^{-1}\mathbf{\Gamma}\mathbf{F}_U, \tag{8}$$

where $\mathbf{\Gamma} \in \mathbb{C}^{RK\times UTK}$ is the corresponding diagonal block matrix, and $\mathbf{F}_R^{-1} = \frac{1}{K}\mathbf{F}_R^\ddagger \in \mathbb{C}^{RK\times RK}$ is the unitary block inverse discrete fourier transform (IDFT) matrix. ‡ indicates the Hermitian transpose, and $\mathbf{F}_R \in \mathbb{C}^{RK\times RK}$ is block-diagonal DFT matrix given by

$$\mathbf{F}_R = \mathbf{I}_R \otimes \mathbf{F} \tag{9}$$

for the R received antennas, where the symbol $\otimes$ indicates the Kronecker product. $\mathbf{F}_U \in \mathbb{C}^{UTK\times UTK}$ is given by

$$\mathbf{F}_U = \mathbf{I}_U \otimes \mathbf{F} \tag{10}$$

for the transmit antennas of all users, where $\mathbf{I}_U \in \mathbb{C}^{UT\times UT}$ is the identity matrix. Average signal-to-noise ratio per receiver antenna is defined as ratio of information bit power and noise power, as

$$\frac{E_b}{N_o} = \frac{P_s}{2\sigma^2 R_c Q U}, \tag{11}$$

where, $P_s = \frac{1}{K}Trace\left\{E\left\{\mathbf{b}\mathbf{b}^\ddagger\right\}\right\}$ is the transmitted symbol energy, Q the number of bits per symbol, and R_c the coding rate, and $E\{\ \}$ defines the expectation over its argument.

III. Iterative Frequency Domain Joint-over-Antenna Multiuser MIMO Detector

The iterative frequency domain JA detector depicted in Fig. 2 exchanges iteratively extrinsic information between two soft input soft output (SfISfO) steps; equalization and channel decoder. The extrinsic information exchange follows the turbo principle, and the aim of the equalization stage is to mitigate ISI and CCI. The equalization stage consists of three stages; soft-cancellation, groupwise filtering, and joint-detection. Correspondingly, the channel decoder's task is to generate soft decisions of the decoded bits in the time domain based on the *a* priori information for the coded bits and on the trellis structure of the constituent codes.

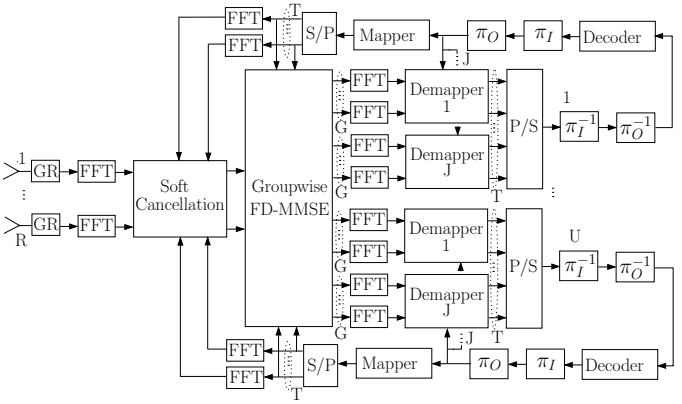

Fig. 2. Iterative frequency domain JA multiuser MIMO detector.

A. Soft-cancellation

In order to detect transmitted layers, soft-cancellation needs to be performed first. The frequency domain residual interference, $\hat{\mathbf{r}} \in \mathbb{C}^{RK\times 1}$, after the cancellation of signal components to be detected from the received signal is given by

$$\hat{\mathbf{r}} = \mathbf{F}_R\mathbf{r} - \mathbf{\Gamma}\mathbf{F}_U\tilde{\mathbf{b}}, \tag{12}$$

where $\tilde{\mathbf{b}} \in \mathbb{C}^{UTK\times 1}$ represents the soft-estimate of the multiple user's transmitted signal vector

$$\tilde{\mathbf{b}} = [\tilde{\mathbf{b}}^1,...,\tilde{\mathbf{b}}^u,...,\tilde{\mathbf{b}}^U]^\dagger \tag{13}$$

with $\tilde{\mathbf{b}}^u \in \mathbb{C}^{TK\times 1}$ being the u^{th} user soft estimate of the transmitted layers

$$\tilde{\mathbf{b}}^u = [\tilde{\mathbf{b}}^{u,1},...,\tilde{\mathbf{b}}^{u,t},...,\tilde{\mathbf{b}}^{u,T}]^\dagger. \tag{14}$$

$\tilde{\mathbf{b}}^{u,t} \in \mathbb{C}^{K\times 1}$ is given by

$$\tilde{\mathbf{b}}^{u,t} = \left[\tilde{b}_1^{u,t}\dots\tilde{b}_k^{u,t}\dots\tilde{b}_K^{u,t}\right]^\dagger \tag{15}$$

with $\tilde{b}_k^{u,t}$ being soft estimate of k^{th} transmitted symbol of the u^{th} user's t^{th} layer. The first two moments of soft-symbol estimates, $\tilde{b}_k^{u,t} = E\left\{b_k^{u,t}\right\}$ and $E\left\{\left|b_k^{u,t}\right|^2\right\}$, are obtained as

$$\tilde{b}_k^{u,t} = E\left\{b_k^{u,t}\right\} = \sum_{b_i\in M} b_i P(b_k^{u,t} = b_i). \tag{16}$$

and

$$E\left\{\left|b_k^{u,t}\right|^2\right\} = \sum_{b_i\in M} |b_i|^2 P(b_k^{u,t} = b_i). \tag{17}$$

respectively, which will be utilized in the next section. The symbol a priori probability $P(b_k^{u,t} = b_i)$ in (16) and (17) can be calculated from [4]

$$P(b_k^{u,t} = b_i) = \left(\frac{1}{2}\right)^Q \prod_{q=1}^{Q}\left(1 + \overline{c}_{i,q}\tanh\left(\lambda_{k,q}^{u,t}/2\right)\right), \tag{18}$$

with $\overline{c}_{i,q} = 2c_{i,q} - 1$ and $\lambda_{k,q}^{u,t}$ being a priori likelihood ratio of the bit $c_{i,q}$, provided by decoder.

B. Frequency Domain Groupwise MMSE Filtering

The groupwise filtering suppresses the u^{th} user's residual ISI components from the symbols within the same transmit antenna group, and the CCI components between different transmit antenna groups and different users. The number of jointly detected antennas, G and the peruser transmit antennas, T, determine the number J of jointly detected antenna groups, as $J = [T/G]$, where $[\,]$ indicates the largest integer smaller than its argument. Note that joint detection over the multiple users is out of the scope of this paper.

1) Exact Solution: The frequency domain groupwise filter coefficients $\mathbf{\Omega}_u^j \in \mathbb{C}^{RK\times GK}$ for the u^{th} user's j^{th} jointly detected antenna group, and the *virtual* channel matrix $\mathbf{A}_u^j \in \mathbb{C}^{GK\times GK}$ of equivalent frequency flat Gaussian channels are determined jointly according to the following MMSE criterion:

$$[\mathbf{\Omega}_u^j, \mathbf{A}_u^j] = \arg\min_{\mathbf{\Omega}_u^j, \mathbf{A}_u^j} E\left\{ \left\| \mathbf{F}_G^{-1}\mathbf{\Omega}_u^{j\,\ddagger}\hat{\mathbf{r}}_u^j - \mathbf{S}(n)\mathbf{A}_u^{j\,\ddagger}\mathbf{b}_u^j \right\|^2 \right\}, \quad (19)$$

where $\mathbf{S}(n) \in \mathbb{R}^{GK\times GK}$ is a time-varying sampling matrix having ones one the main diagonal at the symbol timing of interest, with the rest of the elements being zeros, and $\mathbf{b}_u^j \in \mathbb{C}^{GK\times 1}$ with $j = 1...J$ is the u^{th} user's j^{th} desired group to be jointly detected. $\mathbf{F}_G \in \mathbb{C}^{GK\times GK}$ is defined as $\mathbf{F}_G = \mathbf{I}_G \otimes \mathbf{F}$ with $\mathbf{I}_G \in \mathbb{C}^{G\times G}$ being an identity matrix. The vector $\hat{\mathbf{r}}_u^j \in \mathbb{C}^{RK\times 1}$ combines the soft-cancellation outputs for the desired transmit antenna group, as

$$\hat{\mathbf{r}}_u^j = \hat{\mathbf{r}} + \mathbf{F}_R\hat{\mathbf{H}}_u^j\mathbf{S}(n)\tilde{\mathbf{b}}_u^j, \quad (20)$$

where $\tilde{\mathbf{b}}_u^j \in \mathbb{C}^{GK\times 1}$ is the j^{th} group of the soft estimates of the u^{th} desired user's layers in the group. The block-circulant channel matrix $\hat{\mathbf{H}}_u^j \in \mathbb{C}^{RK\times GK}$ corresponds to the u^{th} desired user's j^{th} transmit antenna group. The *virtual* channel matrix $\mathbf{A}_u^j \in \mathbb{C}^{GK\times GK}$ is given by

$$\mathbf{A}_u^j = \begin{bmatrix} \mathbf{A}^{1,1} & \dots & \mathbf{A}^{1,G} \\ \vdots & \ddots & \vdots \\ \mathbf{A}^{G,1} & \dots & \mathbf{A}^{G,G} \end{bmatrix} \quad (21)$$

with its submatrix $\mathbf{A}^{f,v} \in \mathbb{C}^{K\times K}$, $f, v = 1...G$ being the *virtual* sub-channel matrix between the f^{th} transmit and the v^{th} receive antenna, given by

$$\mathbf{A}^{f,v} = diag\left\{ \left[a_1^{f,v} \dots a_k^{f,v} \dots a_K^{f,v} \right]^\dagger \right\}. \quad (22)$$

The operator $diag\{\ \}$ generates matrix that has the values on the main diagonal. $a_k^{f,v}$ is the path gain of the *virtual* equivalent channel matrix for the k^{th} symbol time instant.

A derivation of the solution to the optimization problem of (19) is provided in Appendix. The MMSE filter coefficients $\mathbf{\Omega}_u^j$, multiplied by DFT matrix $\mathbf{F}_G$, are now found to be given by (76) in Appendix. Note that the square matrix $\mathbf{\Theta}_u^{j,g,g} \in \mathbb{C}^{K\times K}$ in (76) is a sub-matrice of $\mathbf{\Theta}_u^j \in \mathbb{C}^{GK\times GK}$ given by

$$\mathbf{\Theta}_u^j = \dot{\mathbf{B}}_u^{j^{-1}} + \mathbf{\Phi}_u^{j\,\ddagger}\mathbf{\Sigma}_{\hat{r}}^{u,j^{-1}}\mathbf{\Phi}_u^j \quad (23)$$

with $\mathbf{\Sigma}_{\hat{r}}^{u,j} \in \mathbb{C}^{RK\times RK}$ being the covariance matrix of the composite residual and desired signal components, given by

$$\mathbf{\Sigma}_{\hat{r}}^{u,j} = \mathbf{\Sigma}_{\hat{r}} + \mathbf{\Phi}_u^j\breve{\mathbf{\Lambda}}_u^j\mathbf{\Phi}_u^{j\,\ddagger}. \quad (24)$$

$\mathbf{\Phi}_u^j \in \mathbb{C}^{RK\times GK}$, $\breve{\mathbf{\Lambda}}_u^j \in \mathbb{C}^{GK\times GK}$ are, respectively, given by

$$\mathbf{\Phi}_u^j = \mathbf{F}_R\hat{\mathbf{H}}_u^j\mathbf{S}(n) \quad (25)$$

and

$$\breve{\mathbf{\Lambda}}_u^j = diag\left\{ \left[\breve{\mathbf{d}}_u^{j,1} \dots \breve{\mathbf{d}}_u^{j,g} \dots \breve{\mathbf{d}}_u^{j,G} \right]^\dagger \right\}, \quad (26)$$

and the covariance matrix of the residual $\mathbf{\Sigma}_{\hat{r}} \in \mathbb{C}^{RK\times RK}$ by

$$\mathbf{\Sigma}_{\hat{r}} = \mathbf{\Gamma}\mathbf{F}_U\mathbf{\Lambda}\mathbf{F}_U{}^\ddagger\mathbf{\Gamma}^\ddagger + \sigma^2\mathbf{I}, \quad (27)$$

where it has been assumed that the transmitted symbols in the layers are statistically independent.

The soft-feedback terms in (23), (26) and (27) are defined as follows: $\mathbf{B}_u^j \in \mathbb{C}^{GK\times GK}$ in (23) is obtained as

$$\dot{\mathbf{B}}_u^j = diag\left\{ \left[\dot{\mathbf{b}}_u^{j,1} \dots \dot{\mathbf{b}}_u^{j,g} \dots \dot{\mathbf{b}}_u^{j,G} \right]^\dagger \right\}, \quad (28)$$

where $\dot{\mathbf{b}}_u^{j,g} \in \mathbb{C}^{K\times 1}$ is given by

$$\dot{\mathbf{b}}_u^{j,g} = \left[E\left\{ |b_1^{u,j,g}|^2 \right\} \dots E\left\{ |b_k^{u,j,g}|^2 \right\} \dots E\left\{ |b_K^{u,j,g}|^2 \right\} \right]^\dagger, \quad (29)$$

and the second moment of the soft-symbol estimates $E\left\{ |b_k^{u,j,g}|^2 \right\}$ is obtained by utilizing (17). Note that because of the grouping, the indexes with the soft symbols in (17) have to be associated with the user u, group j, and antenna g, which are different from those used in (17). By using (29), $\breve{\mathbf{d}}_u^{j,g} \in \mathbb{C}^{K\times 1}$ in (26) can then be given by

$$\breve{\mathbf{d}}_u^{j,g} = \ddot{\mathbf{b}}_u^{j,g} - \dot{\mathbf{b}}_u^{j,g} \quad (30)$$

with $\ddot{\mathbf{b}}_u^{j,g} \in \mathbb{C}^{K\times 1}$ being

$$\ddot{\mathbf{b}}_u^{j,g} = \left[|\tilde{b}_1^{u,j,g}|^2 \dots |\tilde{b}_k^{u,j,g}|^2 \dots |\tilde{b}_K^{u,j,g}|^2 \right]^\dagger, \quad (31)$$

where soft-symbol estimates $\tilde{b}_k^{u,j,g}$ are obtained using (16).

The diagonal matrix $\mathbf{\Lambda} \in \mathbb{C}^{UTK\times UTK}$ expresses the mean residual interference energy after soft cancellation, as

$$\mathbf{\Lambda} = diag\left\{ \left[\hat{\mathbf{d}}_1 \dots \hat{\mathbf{d}}_u \dots \hat{\mathbf{d}}_U \right]^\dagger \right\}, \quad (32)$$

where $\hat{\mathbf{d}}_u \in \mathbb{C}^{TK\times TK}$ is given by

$$\hat{\mathbf{d}}_u = \dot{\mathbf{b}}_u - \ddot{\mathbf{b}}_u \quad (33)$$

with $\dot{\mathbf{b}}_u \in \mathbb{C}^{TK\times 1}$ being

$$\dot{\mathbf{b}}_u = \left[\dot{\mathbf{b}}^{u,1} \dots \dot{\mathbf{b}}^{u,t} \dots \dot{\mathbf{b}}^{u,T} \right]^\dagger \quad (34)$$

and $\dot{\mathbf{b}}^{u,t} \in \mathbb{C}^{K\times 1}$ obtained in the same way as $\dot{\mathbf{b}}_k^{u,j,g}$ in (29) was obtained. The vector $\ddot{\mathbf{b}}_u \in \mathbb{C}^{TK\times 1}$ in (33) is denoted as

$$\ddot{\mathbf{b}}_u = \left[\ddot{\mathbf{b}}^{u,1} \dots \ddot{\mathbf{b}}^{u,t} \dots \ddot{\mathbf{b}}^{u,T} \right]^\dagger, \quad (35)$$

where $\ddot{\mathbf{b}}^{u,t} \in \mathbb{C}^{K\times 1}$ is obtained in the same way as $\tilde{\mathbf{b}}_k^{u,j,g}$ in (31) was obtained. Note that because of the grouping, the indexes with the soft symbols in (29) and (31) are different from those used in (34) and (35).

The block circulant Hermitian covariance matrix $\mathbf{\Delta} \in \mathbb{C}^{UTK\times UTK}$ of the feedback soft estimates can then be obtained as

$$\mathbf{\Delta} = \mathbf{F}_U\mathbf{\Lambda}\mathbf{F}_U^\dagger. \quad (36)$$

In order to reduce the computational complexity, the matrix inversion lemma [27] is used to invert the covariance matrix of (24), resulting in

$$\mathbf{\Sigma}_{\hat{r}}^{u,j^{-1}}=\mathbf{\Sigma}_{\hat{r}}^{-1}-\mathbf{\Sigma}_{\hat{r}}^{-1}\mathbf{\Phi}_u^j\left(\mathbf{\Phi}_u^{j^\dagger}\mathbf{\Sigma}_{\hat{r}}^{-1}\mathbf{\Phi}_u^j+\breve{\mathbf{\Lambda}}_u^{j^{-1}}\right)^{-1}\mathbf{\Phi}_u^{j^\dagger}\mathbf{\Sigma}_{\hat{r}}^{-1}, \quad (37)$$

Finally, by using (19), (20), (25), (26), (37) and (76) the groupwise MMSE filter output $\mathbf{z}_u^j \in \mathbb{C}^{GK\times 1}$ can be written as

$$\mathbf{z}_u^j = \mathbf{\Xi}_u^{j^{-1}}\mathbf{\Pi}_u^j(\mathbf{S}(n)\mathbf{F}_G^{-1}\mathbf{\Gamma}_u^{j^\dagger}\mathbf{\Sigma}_{\hat{r}}^{-1}\hat{\mathbf{r}}+\mathbf{\Upsilon}_u^j\tilde{\mathbf{b}}_u^j), \quad (38)$$

where $\mathbf{\Upsilon}_u^j \in \mathbb{C}^{GK\times GK}$ is defined as

$$\mathbf{\Upsilon}_u^j = \mathbf{S}(n)\mathbf{F}_G^{-1}\mathbf{\Gamma}_u^{j^\dagger}\mathbf{\Sigma}_{\hat{r}}^{-1}\mathbf{\Gamma}_u^j\mathbf{F}_G\mathbf{S}(n), \quad (39)$$

with which the matrix $\mathbf{\Pi}_u^j \in \mathbb{C}^{GK\times GK}$ in (38) is given by

$$\mathbf{\Pi}_u^j = \mathbf{I}_{GK}-\mathbf{\Upsilon}_u^j(\mathbf{\Upsilon}_u^j+\breve{\mathbf{\Lambda}}_u^{j^{-1}})^{-1}. \quad (40)$$

Now, let $bdiag\{\}$ denote operation to generate block diagonal matrix. $\mathbf{\Xi}_u^j \in \mathbb{C}^{GK\times GK}$ is then expressed as

$$\mathbf{\Xi}_u^j = bdiag\{\mathbf{\Theta}_u^{j,1,1}...\mathbf{\Theta}_u^{j,g,g}...\mathbf{\Theta}_u^{j,G,G}\}, \quad (41)$$

where the square matrix $\mathbf{\Theta}_u^{j,g,g} \in \mathbb{C}^{K\times K}$ is defined by the explanatory sentence before (23). Using (37) the matrix $\mathbf{\Theta}_u^j$ can be re-written as

$$\mathbf{\Theta}_u^j = \dot{\mathbf{B}}_u^{j^{-1}}+\mathbf{\Upsilon}_u^j-\mathbf{\Upsilon}_u^j(\mathbf{\Upsilon}_u^j+\breve{\mathbf{\Lambda}}_u^{j^{-1}})^{-1}\mathbf{\Upsilon}_u^j. \quad (42)$$

It should be noted at this stage since the matrix $\mathbf{\Delta}$ is block circulant Hermitian, the covariance matrix $\mathbf{\Sigma}_{\hat{r}}$ of the residual interference does not have diagonal structure. Therefore, it requires unacceptable computational efforts to strictly invert (27), and to calculate $\mathbf{\Upsilon}_u^j$ as well. Moreover, the sampling matrix, $\mathbf{S}(n)$, still remains in the filter output expression of (38), which necessitates the whole chain of equations for the algorithm to be calculated at every symbol timing.

2) Approximation: To reduce the prohibitive computational complexity for the exact solution, an approximated algorithm is derived in this sub-section. As indicated in previous sub-section, the major computationally complexity is due to matrix inversion of the residual covariance $\mathbf{\Sigma}_{\hat{r}}$. This invokes an idea that $\mathbf{\Delta}$ be approximated by a diagonal matrix. In this paper, we follow the technique presented in [4] that replaces the symbol-wise residual interference energy terms in (33) by each layer's corresponding time-average. With this approximation, the necessity for the symbol-by-symbol computation of the algorithm can be avoided, because the residual interference energy is assumed to be the same over one received frame within each layer. It is shown in [4] that the time-average approximation results in only a minor performance degradation compared to from the exact solution.

With the time-average approximation, $\mathbf{\Delta}$ is replaced by a diagonal matrix

$$\mathbf{\Delta} \approx diag\left\{\left[\overline{\hat{\mathbf{d}}}_1\dots\overline{\hat{\mathbf{d}}}_u\dots\overline{\hat{\mathbf{d}}}_U\right]^\dagger\otimes\mathbf{1}\right\} \quad (43)$$

where $\mathbf{1}\in\mathbb{R}^{K\times 1}$ is a vector having all the elements being one, and $\overline{\hat{\mathbf{d}}}_u \in \mathbb{C}^{T\times 1}$ is defined as

$$\overline{\hat{\mathbf{d}}}_u = \left[\overline{\hat{d}}_u^1\dots\overline{\hat{d}}_u^t\dots\overline{\hat{d}}_u^T\right]^\dagger. \quad (44)$$

The scalar $\overline{\hat{d}}_u^t$ in (44) is given by using (34) and (35) as

$$\overline{\hat{d}}_u^t = avg\left\{\dot{\mathbf{b}}^{u,t}-\ddot{\mathbf{b}}^{u,t}\right\} \quad (45)$$

where the operator $avg\{\}$ calculates the vectorwise average from its argument vector as $avg\{\}=\frac{1}{K}\sum$. With this approximation, significant computational complexity reduction can be expected.

Due to the time-invariance of the residual interference energy over the frame and the necessity of using the sampling matrix $\mathbf{S}(n)$ can be now eliminated. Substituting (43) into (27) the groupwise MMSE filter output of (38) can be re-written as

$$\mathbf{z}_u^j = \mathbf{\Xi}_u^{j^{-1}}\mathbf{\Pi}_u^j(\mathbf{F}_G^{-1}\mathbf{\Gamma}_u^{j^\dagger}\mathbf{\Sigma}_{\hat{r}}^{-1}\hat{\mathbf{r}}+\mathbf{\Upsilon}_u^j\tilde{\mathbf{b}}_u^j), \quad (46)$$

where $\mathbf{\Gamma}_u^j \in \mathbb{C}^{RK\times GK}$ is obtained by applying (8) with $\mathbf{F}_G$ to $\hat{\mathbf{H}}_u^j$. With the diagonal structure of $\mathbf{\Delta}$, the matrices $\mathbf{\Upsilon}_u^j$ and $\mathbf{\Pi}_u^j$ in (39) and (40), respectively, can be re-written as

$$\mathbf{\Upsilon}_u^j = \begin{bmatrix}\varphi_u^{1,1}\mathbf{I}_K & \dots & \varphi_u^{1,G}\mathbf{I}_K\\ \vdots & \ddots & \vdots\\ \varphi_u^{G,1}\mathbf{I}_K & \dots & \varphi_u^{G,G}\mathbf{I}_K\end{bmatrix}, \quad (47)$$

and

$$\mathbf{\Pi}_u^j = \mathbf{I}_{GK}-\mathbf{\Upsilon}_u^j(\mathbf{\Upsilon}_u^j+\overline{\breve{\mathbf{\Lambda}}}_u^{j^{-1}})^{-1} \quad (48)$$

where $\mathbf{I}_{GK}\in\mathbb{R}^{GK\times GK}$ is an identity matrix. The scalar $\varphi_u^{g,f}$, $f=1,\dots,G$, in (47) is given by [2]

$$\varphi_u^{g,f} = \frac{1}{K}Trace\left\{\mathbf{\Gamma}_{u,j}^{g^\dagger}\mathbf{\Sigma}_{\hat{r}}^{-1}\mathbf{\Gamma}_{u,j}^f\right\}, \quad (49)$$

where the matrix $\mathbf{\Gamma}_{u,j}^g \in \mathbb{C}^{RK\times K}$ presents the frequency domain channel matrix of the gth transmit antenna in the j^{th} group.

The matrix $\mathbf{\Xi}_u^j$ calculated by using (41), of which the sub-matrices $\mathbf{\Theta}_u^{j,g,g}$ yielding the matrix $\mathbf{\Theta}_u^j$ given by (42) can now be re-written as

$$\mathbf{\Theta}_u^j = \overline{\dot{\mathbf{B}}}_u^{j^{-1}}+\mathbf{\Upsilon}_u^j-\mathbf{\Upsilon}_u^j(\mathbf{\Upsilon}_u^j+\overline{\breve{\mathbf{\Lambda}}}_u^{j^{-1}})^{-1}\mathbf{\Upsilon}_u^j, \quad (50)$$

where $\overline{\dot{\mathbf{B}}}_u^j \in \mathbb{C}^{GK\times GK}$ are computed by using (28) as

$$\overline{\dot{\mathbf{B}}}_u^j = diag\left\{\left[avg\left\{\dot{\mathbf{b}}_u^{j,1}\right\}\dots avg\left\{\dot{\mathbf{b}}_u^{j,g}\right\}\dots avg\left\{\dot{\mathbf{b}}_u^{j,G}\right\}\right]^\dagger\otimes\mathbf{1}\right\}. \quad (51)$$

The matrix $\overline{\breve{\mathbf{\Lambda}}}_u^j \in \mathbb{C}^{GK\times GK}$ in (48) can be computed by using (30) as

$$\overline{\breve{\mathbf{\Lambda}}}_u^j = diag\left\{\left[avg\left\{\breve{\mathbf{d}}_u^{j,1}\right\}\dots avg\left\{\breve{\mathbf{d}}_u^{j,g}\right\}\dots avg\left\{\breve{\mathbf{d}}_u^{j,G}\right\}\right]^\dagger\otimes\mathbf{1}\right\}. \quad (52)$$

Note that the square matrix $\mathbf{\Theta}_u^{j,g,g}\in\mathbb{C}^{K\times K}$ is defined by the explanatory sentence before (23).

[2] Note that only diagonal entries of each sub-matrice in (39) have to be considered, because of the sampling matrix **S**(n).

C. Equivalent AWGN Channel Model

It is well known that the distribution of residual interference-plus-noise at the output of the MMSE filter (46) can be approximated as being Gaussian-distributed [28]. Therefore, it is reasonable for the SfISfO channel decoder to assume that the soft output of MMSE filter represents the output of an equivalent AWGN channel having $\mathbf{b}_u^j$ as an input to the channel [6]. Therefore, the output of the MMSE filter (46) can be re-written as follows:

$$\mathbf{z}_u^j = \mathbf{\Phi}_u^j \mathbf{b}_u^j + \mathbf{v}_u^j, \tag{53}$$

where the gains of equivalent Gaussian channel $\mathbf{\Phi}_u^j \in \mathbb{C}^{GK\times GK}$ are expressed as

$$\mathbf{\Phi}_u^j = \mathbf{\Xi}_u^{j^{-1}} \mathbf{\Pi}_u^j \mathbf{\Upsilon}_u^j. \tag{54}$$

The vector $\mathbf{v}_u^j \in \mathbb{C}^{GK\times 1}$ represents the noise components of the equivalent Gaussian channel with zero mean and variance $\mathbf{\Psi}_u^j \in \mathbb{C}^{GK\times GK}$ expressed as

$$\mathbf{\Psi}_u^j = \mathbf{\Xi}_u^{j^{-1}} \mathbf{\Pi}_u^j (\dot{\mathbf{\Upsilon}}_u^j + \ddot{\mathbf{\Upsilon}}_u^j) \mathbf{\Pi}_u^{j^\ddagger} \mathbf{\Xi}_u^{j^{-1}}. \tag{55}$$

The matrix $\dot{\mathbf{\Upsilon}}_u^j \in \mathbb{C}^{GK\times GK}$ is defined as

$$\dot{\mathbf{\Upsilon}}_u^j = \begin{bmatrix} \dot{\varphi}_u^{1,1}\mathbf{I}_K & \dots & \dot{\varphi}_u^{1,G}\mathbf{I}_K \\ \vdots & \ddots & \vdots \\ \dot{\varphi}_u^{G,1}\mathbf{I}_K & \dots & \dot{\varphi}_u^{G,G}\mathbf{I}_K \end{bmatrix} \tag{56}$$

with $\dot{\varphi}_u^{g,f}$ being [3]

$$\dot{\varphi}_u^{g,f} = \frac{1}{K} Trace\left\{ \mathbf{\Gamma}_{u,j}^{g^\ddagger} \mathbf{\Sigma}_{\hat{r}}^{-1} \mathbf{\Gamma} \mathbf{\Delta} \mathbf{\Gamma}^\ddagger \mathbf{\Sigma}_{\hat{r}}^{-1} \mathbf{\Gamma}_{u,j}^f \right\}, \tag{57}$$

and $\ddot{\mathbf{\Upsilon}}_u^j \in \mathbb{C}^{GK\times GK}$ defined as

$$\ddot{\mathbf{\Upsilon}}_u^j = \begin{bmatrix} \ddot{\varphi}_u^{1,1}\mathbf{I}_K & \dots & \ddot{\varphi}_u^{1,G}\mathbf{I}_K \\ \vdots & \ddots & \vdots \\ \ddot{\varphi}_u^{G,1}\mathbf{I}_K & \dots & \ddot{\varphi}_u^{G,G}\mathbf{I}_K \end{bmatrix} \tag{58}$$

with $\ddot{\varphi}_u^{g,f}$ being [3]

$$\ddot{\varphi}_u^{g,f} = \frac{\sigma^2}{K} Trace\left\{ \mathbf{\Gamma}_{u,j}^{g^\ddagger} \mathbf{\Sigma}_{\hat{r}}^{-1} \mathbf{\Sigma}_{\hat{r}}^{-1} \mathbf{\Gamma}_{u,j}^f \right\}. \tag{59}$$

D. MAP Detector

The joint detection of transmitted layers of each user is performed by using a MAP detector. The MAP detector given in [12] aims to decouple the transmitted layers within the same group to be jointly detected. The MAP detector is denoted in Fig. 2 as de-mapper, because it performs also symbol-to-soft bit conversion. Since the MAP algorithm itself is very well-known [1][29], its details are not given but only necessary equations are provided in this section. Let us introduce distance metric needed in MAP algorithm which in [12]:

$$\zeta_{u,j}^{k,s,w} = (\vec{\mathbf{z}}_u^{j,k} - \vec{\mathbf{\Phi}}_u^{j,k} \mathfrak{M}\{\dot{\mathbf{c}}_w\})^\ddagger \vec{\mathbf{\Psi}}_u^{j,k^{-1}} (\vec{\mathbf{z}}_u^{j,k} - \vec{\mathbf{\Phi}}_u^{j,k} \mathfrak{M}\{\dot{\mathbf{c}}_w\}) \tag{60}$$

with $w = 1\cdots 2^{GQ}$ and $s = 1\cdots GQ$. Let's define the operator $\vec{}$ that extracts the elements from its argument vector and/or matrix, all of which correspond to the kth symbol time instant. By using (46) the equalizer output for the kth symbol time instant is defined as $\vec{\mathbf{z}}_u^{j,k} \in \mathbb{C}^{G\times 1}$. Recall that the matrix $\mathbf{\Phi}_u^j$ has entries corresponding to the equivalent channel coefficients. The gain matrix of $\vec{\mathbf{\Phi}}_u^{j,k} \in \mathbb{C}^{G\times G}$ of the equivalent AWGN channel for the kth symbol time instant can be derived in the same way as the global channel matrix (54) was obtained. The covariance matrix of equivalent of AWGN component $\vec{\mathbf{\Psi}}_u^{j,k} \in \mathbb{C}^{G\times G}$ for the kth symbol timing can be derived also in the similar way to deriving the global covariance matrix in Eq. (55). $\mathfrak{M}\{\}$ is mapping function for the bit-to-symbol conversion, and $\dot{\mathbf{c}}_w$ is the w^{th} candidate bit vector. Using Eq. (60), the extrinsic Log-likelihood ratio (LLR) $\lambda_{k,s}^{u,j}$ of the sth bit constituting the kth symbol of the uth user, derived from the extrinsic probability, is given by

$$\lambda_{k,s}^{u,j} = ln \frac{\sum_{\forall c_{w,s}=1} e^{(-\zeta_{u,j}^{k,s,w} + \sum_{s\prime\neq s} lnP(c_{k,s\prime}^{u,j}))}}{\sum_{\forall c_{w,s}=0} e^{(-\zeta_{u,j}^{k,s,w} + \sum_{s\prime\neq s} lnP(c_{k,s\prime}^{u,j}))}}, \tag{61}$$

where $s\prime = 1\cdots GQ$, and $lnP(c_{k,s\prime}^{u,j})$ is the natural logarithm of a priori probabilities of the coded bits. Now, depending on the value of the bit being zero or one, the a priori probabilities of the coded bits $lnP(c_{k,s\prime}^{u,j} = 0)$ and $lnP(c_{k,s\prime}^{u,j} = 1)$, respectively, are calculated in the similar way to that shown in [29], respectively, as

$$lnP(c_{k,s\prime}^{u,j} = 1) = \lambda_{k,s\prime}^{u,j} - ln(1 + e^{\lambda_{k,s\prime}^{u,j}}) \tag{62}$$

and

$$lnP(c_{k,s\prime}^{u,j} = 0) = -ln(1 + e^{\lambda_{k,s\prime}^{u,j}}). \tag{63}$$

$c_{w,s} = 1$ and $c_{w,s} = 0$ correspond to the candidate vectors having one or zero, respectively, at the s^{th} position. It should be also noted that in the computation of numerator and denominator for Eq. (61) the Jacobian algorithm can be used as in [29].

IV. Complexity Analysis

In this section computational complexities of the frequency domain (FD) and the time domain (TD) JA detectors are evaluated based on the mathematical expressions given in this paper and in [12], respectively. In the both FD and TD cases the complexity evaluation include MMSE and MAP algorithms. In the calculation it is also assumed that the manipulations for mean and variance calculations of the equivalent AWGN channel is counted as a part of MMSE filtering. Moreover, the manipulations for the mean and variance calculations of the soft feedback are also taken into account. It is assumed that the TD channel state information is transformed into the frequency domain using FFT. Moreover, it is assumed that matrix inversions are computed by utilizing LU decomposition similar to [30]. However, it should also be noticed that the complexity assessment excludes the mathematical manipulations for the $tanh()$ and $ln()$ functions in the both FD and TD cases.

The approximate count of complex operations per iteration is presented for the TD and FD receivers in Table I. The results demonstrate that the significant complexity reduction can be achieved with FD processing compared to TD processing. The complexity reduction is due mainly to the efficient

[3] same reason as given in [2].

TABLE I

THE NUMBERS OF COMPLEX OPERATIONS FOR ITERATIVE FREQUENCY AND TIME DOMAIN RECEIVERS PER ITERATION.

Per frame

Algorithm	Addition	Multiplication	Division
$FD-MMSE$	$G^3UJ(4+5/6)$ $+5G^2UJ+G(4UJ+1/6)$	$G^3UJ(4+5/6)$ $+5/6UJG$	$UJG(G+2)$
MAP for FD	$UJ(5/6G^3-G^2+G/6)$ $+2^{GQ}UJ(G^2-G)$	$UJ(5/6G^3-5/6G)$ $+2^{GQ}UJG^2$	UJG^2

Per symbol

Algorithm	Addition	Multiplication	Division
$FD-MMSE$	$5/6R^3$ $+6R^2(UJG^2+UJG+UT-1)$ $+R((UT)^2+UT+UJG+1/6)$ $+UJG^3-UJG^2$ $-4UJG+UT(M-1)$	$5/6R^3$ $+R^2(UT+3UJG+1)$ $+R(3UJG+(UT)^2+UT$ $+UJG-5/6)$ $+6U(TM(2Q+2)+TM)$	R^2
MAP for FD	$2^{GQ}UJ(G^2-G)$	$2^{GQ}2UJG^2$	
FFT	$2Rlog_2K+2UTlog_2K$ $+UJGlog_2K$	$Rlog_2K+UTlog_2K$ $+1/2UJGlog_2K$	
$TD-MMSE$	$UJ(5/6(LR)^3$ $+(LR)^2(UT(2L-1)+G)$ $+LR(2G^2-2+1/6$ $+(UT(2L-1)-1)$ $\cdot UT(2L-1)+2UTL-UT)$ $+UT((2L-1)+(2L-1)M))$	$UJ(5/6(LR)^3$ $+(LR)^2(UT(2L-1)+3G)$ $+LR(UT(2L-1)+(UT(2L-1))^2$ $+2G^2+G-5/6)$ $+UT(2L-1)(1+Q)+G^3)$	UJ $\cdot(LR)^2$
MAP for TD	$UJ(5/6G^3-G^2+G/6)$ $+2^{GQ}UJ(3G^2-2G)$	$UJ(5/6G^3-5/6G)$ $+2^{GQ}UJ2G^2$	UJG^2

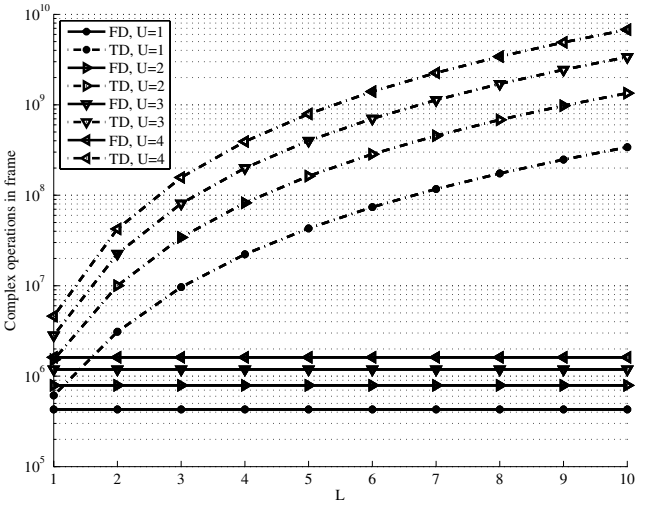

Fig. 3. Computational complexity comparison for TD-JA and FD-JA detectors (Dashed lines TD, solid lines FD) when $U = 1...4, R = 4, T = 2, G = 2, K = 512$.

implementation of MMSE filtering in the frequency domain. However, it should be noticed that MAP algorithm starts to dominate the complexity when the product of GQ becomes large. As a result, the relative complexity difference between FD and TD algorithms becomes smaller but the reduction is still large enough to utilize the FD processing. The total number of complex arithmetic operations is summarized Fig. 3 for $K = 512$, $M = 4$, $U = 4$, $T = G = 2$ and $R = 4$. As can be seen, significant complexity reduction can be achieved with the frequency domain processing compared to the time domain processing.

V. SIMULATION RESULTS

In this section, results of series of Monte-Carlo simulations conducted to evaluate performances of the proposed FD JA multiuser MIMO detector are presented. A synchronous coherent uplink communication system with perfect channel state information at the receiver is considered. The performance measure is frame-error rate (FER) versus average E_b/N_o defined by (11) in frequency-selective Rayleigh fading channels. For the reliability of the results, encoded frames were transmitted until 100 frame errors were counted up for each E_b/N_o value.

The tapped delay line channel model of (7) was assumed, where each of the taps was assumed to have equal average power. Quasistatic fading was assumed, where the channel is constant over frame but changes independently frame by frame. Two different spatial correlation setups were investigated at the transmitter side: One is the uncorrelated case where transmit antenna correlation coefficients α between the consecutive elements is zero; The other highly correlated case where the correlation coefficient $\alpha = 0.9$. The correlation cofficient α correspond the off-diagonal components of spatial correlation matrix similarly as in [31]. The spatial correlation model follows well-known Kronecker model given in [32]. All other relevant simulation parameters are summarized in Table II. As can be seen from Fig. 2 symbol-level as well as bit-level de-interleaving, referred to as π_I^{-1} and π_O^{-1}, respectively, in the figure is performed in succession after spatial MAP, which are corresponding to the interleavers π_I and π_O, at the transmitter, respectively.

It is well-known that SC-MMSE receiver reduces to a channel matched filter if perfect a priori information is available of the all user's transmitted bits at the receiver [33] and all the

TABLE II
SIMULATION PARAMETERS.

Parameter	Value
K	512
P	32
T	$2, 3, 4$
R	$1, 2, 3, 4$
U	$1, 2, 3, 4$
L	32
G	$1, 2, 3, 4$
Q	2 (QPSK)
Turbo encoder	two parallel concatenated recursive systematic convolutional codes (CC)
Turbo encoder interleaver	random interleaver
Turbo encoder polynomials for CC	(1,15,13) in octal [36] with constraint length of three
Turbo encoder puncturing & rate	parity bits are punctured to result $R_c = 1/2$
Symbol-level interleaver	random, 480 symbols
Bit-level interleaver	random, 960 bits
Turbo decoder	Log-MAP algorithm with 8 iterations
Equalizer iterations, E	6 for both AA $(G = 1)$ and JA $(G > 1)$

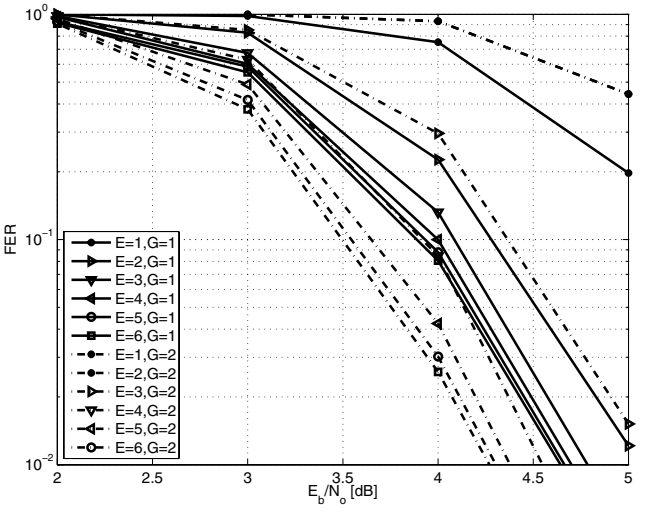

Fig. 4. FER performance of JA and AA receivers for $U = 1, T = R = 2, \alpha = 0.0$ (JA dashed lines, AA solid lines)

interference is canceled. Therefore, upper bound performance (=smallest FER), referred to as matched filter bound (MFB), of the receiver can be obtained by assuming perfect decoder feedback.[4]

A. Single User Results

Figure 4 shows FER performance of the system with a balanced antenna configuration $T = R = 2$ with the different number E of the equalizer iterations. The results show that AA has faster convergence when $E \leq 3$. However, JA achieves more iteration gain with $E > 3$ than AA. A similar phenomenons are also observed in the case of higher numbers of transmit and receive antennas. Figure 5 presents FER performance of AA $(G = 1)$ and JA $(G > 1)$ with the antenna correlation factor as a parameter. It is found that both AA and JA suffers around 1.5 dB loss from MFB when antennas are uncorrelated. The results show that when feedback is reliable enough the performance difference between the two detectors is very minor. In fact, when soft-feedback is perfect soft-cancellation works perfectly and the both detectors have equivalent performance. However, in the presence of spatial correlation AA can not separate the transmitted layers by using MMSE filter as effectively as JA can by using MAP. Since JA detector convergences asymptotically to MFB the presented results also support main outcome of [35] that spatial correlation causes only E_b/N_o loss (parallel shift) but no diversity order degradation when maximum likelihood based receiver is utilized in MIMO transmission. It is expected that the gain achieved by using JA becomes larger when the spatial correlation as well as the number transmitter antennas increase.

Figure 6 shows FER performance in an overloaded antenna configuration. The results show clearly that JA outperforms AA significantly when $T > R$. The performance of AA degrades due to the lack of DoF for MMSE filtering to suppress interference caused by overloaded transmit antennas. The impact of additional preserved DoF is significant, as shown in the figure with $T = 4$, $R = 2$, and $G = 1, 2, 4$, when the number of jointly detected antennas increases. As a result, it is expected that the performance gain by using JA becomes larger when the number of jointly detected antennas becomes larger. The additional DoF for the MMSE filtering are particularly beneficial when soft-feedback is not reliable enough to perform effective soft-cancellation. Correspondingly, by looking at the figure it is found that the performance of JA is degraded, however the diversity order (= corresponding to the decay of the curves) remains the same in all the overloaded cases tested as in the balanced cases. JA's capability of maintaining the equivalent diversity order is due to fact that MMSE can suppress residual ISI after soft-cancellation effectively, while still preserves enough DoF to

[4]Some alternative techniques that are not based on the turbo concept, e.g., Genetic-Algorithm-assisted [34], may achieve comparable performance. However, system assumptions used in those papers are not consistent enough to make fair comparison. Therefore, making comparison between the techniques based on different technological bases is out of the scope of this paper.

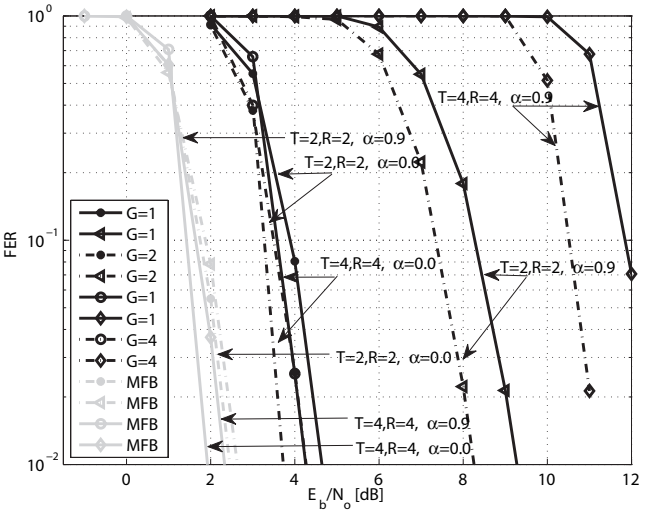

Fig. 5. FER performance of JA and AA receivers for $U = 1$ (JA dashed lines, AA solid lines)

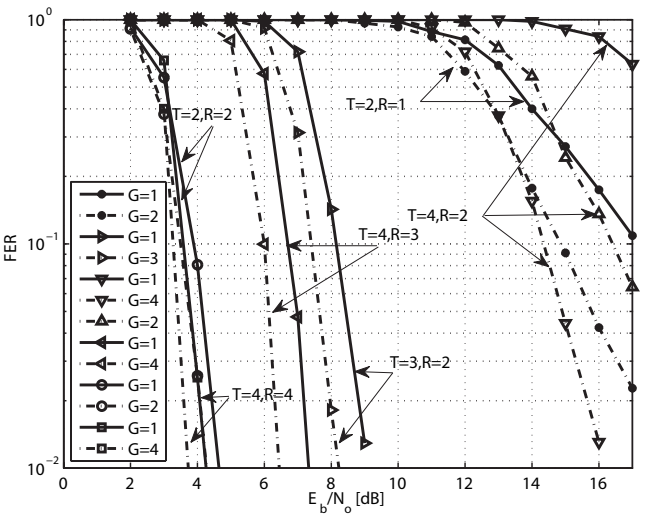

Fig. 6. FER performance of JA and AA receivers for $U = 1, \alpha = 0.0$ (JA dashed black lines, AA solid black lines)

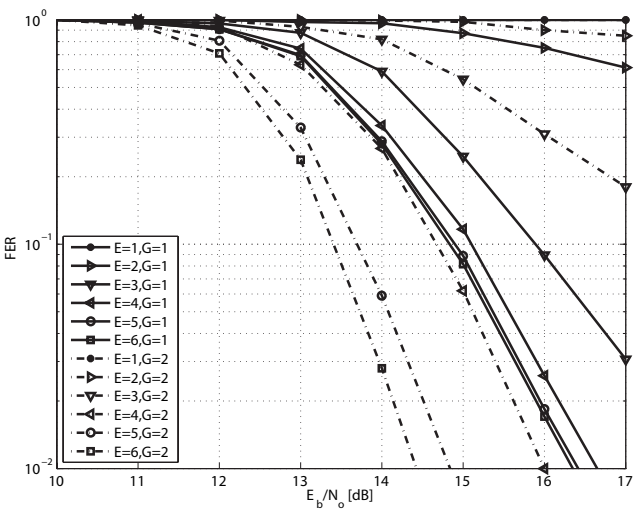

Fig. 7. FER performance of JA and AA receivers for $U = 4, T = 2, R = 4, \alpha = 0.0$ and $\alpha = 0.0$ (JA dashed black lines, AA solid black lines).

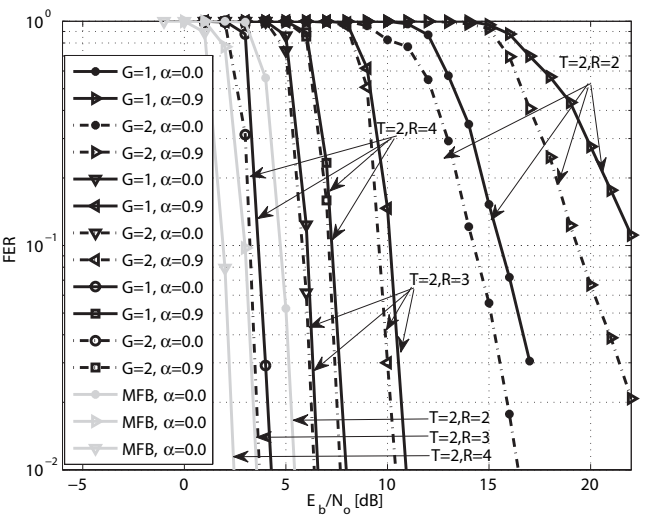

Fig. 8. FER performance of JA and AA receivers for $U = 2, T = 2$ and $R = 2, 3, 4$ (JA dashed black lines, AA solid black lines).

combine the desired signals multipath components.

B. Multiuser Results

Figure 7 depicts FER performance of the system with a balanced antenna configuration $UT = R = 4$ with the different number of equalizer iterations E. A similar tendency in performance curves to Fig. 4's single user case is observed that AA has faster convergence when $E \leq 3$. But, larger iteration gain is achieved with JA for $E > 3$ than AA. Figure 8 depicts FER performance with AA and JA for $U = 2$ with the antenna correlation factor α and the number of receive antennas R as parameters. The performance difference between AA and JA detectors is neglible when $R = 4$ and $\alpha = 0.0$. This is because of the same reason as that discussed in the single user's case. Similarly to the single user case, it should be noticed that spatial correlation does not have any impact on the diversity order but it causes only parallel shift in terms of E_b/N_o. Figure 9 shows FER performance for U = 2,3,4 with $\alpha = 0$ and $\alpha = 0.9$. As can be seen, the larger the difference between UT and R values ($UT \geq R$) the larger gaps between the JA and AA performance curves. This is again because of the same reason as that discussed in the single user's case.

VI. Conclusions

A new iterative frequency domain joint over-antenna multiuser MIMO signal detection technique has been proposed for broadband multiuser MIMO uplink transmission in frequency-selective channels. The proposed frequency domain multiuser MIMO detection technique requires much lower computational complexity than its time-domain counterpart. The results show that significant performance gains can be achieved with JA compared to AA when $UT > R$ and in the presence of spatial correlation. It has also been shown that the computational complexity with the FD algorithm is always lower than TD, and the significance of complexity reduction depends on the system setup as well as channel conditions. Conversely, the significance of performance gain due to the FD algorithm over

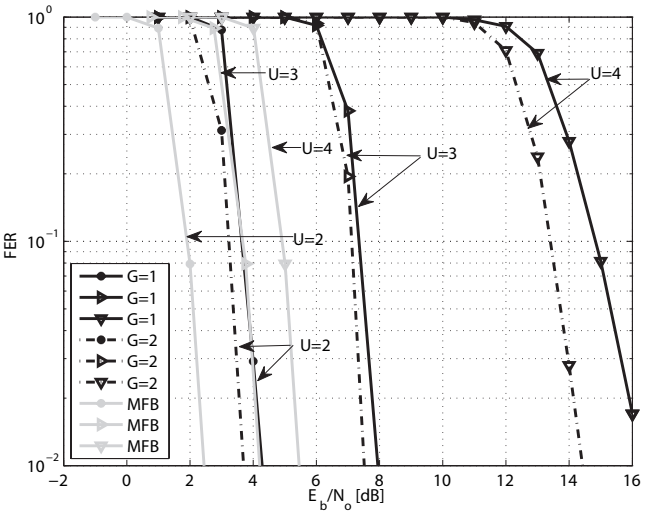

Fig. 9. FER performance of JA and AA receivers for $U = 2, 3, 4, T = 2, R = 4$ and $\alpha = 0.0$ (JA dashed black lines, AA solid black lines)

TD also depends on the system setup and channel conditions. Those observations lead to a conclusion that with a marginal loss in performance the complexity with an FD receiver can be made much lower than another FD receiver having exactly the same parameter setting as its time-domain counterpart in certain scenarios. This may invoke reasonable performance-complexity trade-off when practical applications of the FD algorithm is considered. For this purpose, performance of the TD of JA techniques has to be evaluated, for which however simulation times is already prohibitively long in messy multipath environments.

APPENDIX
THE OPTIMIZATION OF FILTER COEFFICIENTS

The optimisation problem of (19) can be re-written as

$$[\mathbf{\Omega}_u^j, \mathbf{A}_u^j] = \arg \min_{\mathbf{\Omega}_u^j, \mathbf{A}_u^j} E\left\{ \left\| \mathbf{G}_u^{j\,\ddagger} \mathbf{y}_u^j \right\|^2 \right\}, \tag{64}$$

where $\mathbf{G}_u^{j\,\ddagger} \in \mathbb{C}^{GK \times (R+G)K}$ is given by

$$\mathbf{G}_u^{j\,\ddagger} = \left[\begin{array}{cc} \mathbf{F}_G^{-1} \mathbf{\Omega}_u^{j\,\ddagger} & -\mathbf{S}(n) \mathbf{A}_u^{j\,\ddagger} \end{array} \right], \tag{65}$$

and $\mathbf{y}_u^j \in \mathbb{C}^{(R+G)K \times 1}$ by

$$\mathbf{y}_u^j = \left[\begin{array}{c} \hat{\mathbf{r}}_u^j \\ \mathbf{b}_u^j \end{array} \right]. \tag{66}$$

$\mathbf{\Omega}_u^j$ and $\mathbf{A}_u^j$ are subject to a constraint in order to avoid the trivial solution $[\mathbf{\Omega}_u^j, \mathbf{A}_u^j] = [\mathbf{0}, \mathbf{0}]$. Following [12], the path constraint

$$\mathbf{Q}^{g\dagger} \mathbf{G}_s^{j,u,g} = -\mathbf{I}_K \tag{67}$$

is imposed in this paper, where the matrix $\mathbf{Q}^{g\dagger} \in \mathbb{R}^{K \times (R+G)K}$ is given by

$$\mathbf{Q}^{g^\dagger} = \left[\mathbf{0}_{K \times (RK+(g-1)K)} \; \mathbf{I}_K \; \mathbf{0}_{K \times (G-g)K} \right] \tag{68}$$

with $\mathbf{I}_K \in \mathbb{R}^{K \times K}$ being an identity matrix, and $\mathbf{0}_{K \times (RK+(g-1)K)} \in \mathbb{R}^{K \times (RK+(g-1)K)}$ and $\mathbf{0}_{K \times (G-g)K} \in \mathbb{R}^{K \times (G-g)K}$ being zero matrices with the sizes indicated by their dimensionality identifiers. $\mathbf{G}_s^{j,u,g}$ contains all rows from the $(g-1)K+1$-th to gK-th columns in $\mathbf{G}_u$.

The objective function for (64)'s optimization problem can be expressed as a sum of the component cost functions, as

$$\mathcal{J}(\mathbf{G}_s^{j,u,g}) = E\left\{ \sum_{g=1}^{G} Trace\{ \mathbf{G}_s^{j,u,g^\ddagger} \mathbf{\Sigma}_y^{j,u} \mathbf{G}_s^{j,u,g} \} \right\} \tag{69}$$

Since $\mathbf{\Sigma}_y^{j,u}$ is positive semidefinite, the objective function is convex. Thus, the solution to this optimisation problem can be obtained by using the Lagrange method. The cost function equivalent to (69) is re-defined as

$$\mathcal{L}(\mathbf{G}_s^{j,u,g}, \mathbf{L}_{g,u}^j) = \sum_{g=1}^{G} Trace\{ \mathbf{G}_s^{j,u,g^\ddagger} \mathbf{\Sigma}_y^{j,u} \mathbf{G}_s^{j,u,g} \}$$
$$+ \sum_{g=1}^{G} Re\{ Trace\{ \mathbf{L}_{g,u}^\ddagger (\mathbf{Q}^{g^\dagger} \mathbf{G}_s^{j,u,g} + \mathbf{I}_K) \} \}, \tag{70}$$

where the Lagrange multipliers are introduced in diagonal matrices $\mathbf{L}_{g,u} \in \mathbb{C}^{K \times K}$. With the notation above, finding the optimal solution to (70) is equivalent to obtaining the solutions for each of the component cost functions, indexed by g, separately. Therefore, the optimization process is shown only for the g^{th} component cost function, below. By using $Re\{\mathbf{X}\} = \frac{1}{2}(\mathbf{X} + \mathbf{X}^\ddagger)$, the derivatives of the equivalent cost function given by (70) with respect to $\mathbf{G}_s^{j,u,g^\ddagger}$ and $\mathbf{L}_{g,u}$ are obtained as

$$\frac{\partial L(\mathbf{G}_s^{j,u,g}, \mathbf{L}_{g,u})}{\partial \mathbf{G}_s^{j,u,g^\ddagger}} = 2\mathbf{\Sigma}_y^{j,u} \mathbf{G}_s^{j,u,g} + \mathbf{Q}^g \mathbf{L}_{g,u} \tag{71}$$

and

$$\frac{\partial L(\mathbf{G}_s^{j,u,g}, \mathbf{L}_{g,u})}{\partial \mathbf{L}_{g,u}^\ddagger} = \mathbf{Q}^{g^\dagger} \mathbf{G}_s^{j,u,g} + \mathbf{I}_K, \tag{72}$$

respectively. Now, by setting those derivatives equal to zero, $\mathbf{L}_{g,u}$ and $\mathbf{G}_s^{j,u,g}$ that yield the optimal solution are determined as

$$\mathbf{L}_{g,u} = 2(\mathbf{Q}^{g^\dagger} \mathbf{\Sigma}_y^{j,u^{-1}} \mathbf{Q}^g)^{-1} \tag{73}$$

and

$$\mathbf{G}_s^{j,u,g} = -\mathbf{\Sigma}_y^{j,u^{-1}} \mathbf{Q}^g (\mathbf{Q}^{g^\dagger} \mathbf{\Sigma}_y^{j,u^{-1}} \mathbf{Q}^g)^{-1}, \tag{74}$$

respectively, where $\mathbf{\Sigma}_y^{u,j^{-1}}$ is obtained by utilising the block-matrix inversion Lemma [27] , as

$$\mathbf{\Sigma}_y^{u,j^{-1}} = \left[\begin{array}{cc} \mathbf{\Sigma}_{\hat{r}}^{u,j^{-1}} & -\mathbf{\Sigma}_{\hat{r}}^{u,j^{-1}} \mathbf{\Phi}_u^j \\ -\dot{\mathbf{B}}_u^j \dot{\mathbf{B}}_u^{j\,\ddagger} \mathbf{\Phi}_u^{j\,\ddagger} \mathbf{\Sigma}_{\hat{r}}^{u,j^{-1}} & \mathbf{\Theta}_u^j \end{array} \right] \tag{75}$$

with $\mathbf{\Theta}_u^j \in \mathbb{C}^{GK \times GK}$ defined by (23).

By using (74) and (75) the filter coefficients $\mathbf{\Omega}_u^j$ with $\mathbf{F}_G$ and $\mathbf{A}_u^j$ with $\mathbf{S}(n)$ can be obtained as (76) and (77) respectively, where $\mathbf{\Theta}_u^{j,g,g} \in \mathbb{C}^{K \times K}$ is a sub-matrix of $\mathbf{\Theta}_u^j$.

ACKNOWLEDGMENT

The authors would like to thank anonymous reviewers whose comments have significantly improved the paper. They wish also to thank M. Codreanu for valuable discussions on optimization.

$$\mathbf{\Omega}_u^j \mathbf{F}_G = \left[\mathbf{\Sigma}_{\hat{r}}^{u,j^{-1}} \mathbf{\Phi}_u^{j,1} (\mathbf{\Theta}_u^{j,1,1})^{-1} \dots \mathbf{\Sigma}_{\hat{r}}^{u,j^{-1}} \mathbf{\Phi}_u^{j,g} (\mathbf{\Theta}_u^{j,g,g})^{-1} \dots \mathbf{\Sigma}_{\hat{r}}^{u,j^{-1}} \mathbf{\Phi}_u^{j,G} (\mathbf{\Theta}_u^{j,G,G})^{-1} \right] \tag{76}$$

$$-\mathbf{A}_u^j \mathbf{S}(n) = \begin{bmatrix} -\mathbf{\Theta}_u^{j,1,1}(\mathbf{\Theta}_u^{j,1,1})^{-1} & \dots & -\mathbf{\Theta}_u^{j,1,g}(\mathbf{\Theta}_u^{j,g,g})^{-1} & \dots & -\mathbf{\Theta}_u^{j,1,G}(\mathbf{\Theta}_u^{j,G,G})^{-1} \\ \vdots & \dots & \vdots & \dots & \vdots \\ -\mathbf{\Theta}_u^{j,G,1}(\mathbf{\Theta}_u^{j,1,1})^{-1} & \dots & -\mathbf{\Theta}_u^{j,G,g}(\mathbf{\Theta}_u^{j,g,g})^{-1} & \dots & -\mathbf{\Theta}_u^{j,G,G}(\mathbf{\Theta}_u^{j,G,G})^{-1} \end{bmatrix} \tag{77}$$

REFERENCES

[1] C. Berrou, A. Glavieux, and P. Thitimajshima, "Near Shannon limit error correcting coding and decoding," in *Proc. IEEE Int. Conf. Commun. (ICC)*, vol. 2, May 1993, pp. 1064–1070.

[2] C. Douillard, C. M. Jezequel, C. Berrou, A. Picart, P. Didier, and A. Glavieux, "Iterative correction of intersymbol interference: turbo-equalisation," *European Trans. Telecommun.*, vol. 6, no. 5, pp. 507–511, Sept. 1995.

[3] S. L. Ariyavisitakul, "Turbo space-time processing to improve wireless channel capacity," *IEEE Trans. Commun.*, vol. 48, no. 8, pp. 1347–1359, Aug. 2000.

[4] M. Tüchler, A. C. Singer, and R. Koetter, "Minimum mean squared error equalisation using a priori information," *IEEE Trans. Signal Processing*, vol. 50, no. 3, pp. 673–683, Mar. 2002.

[5] R. Koetter, A. Singer, and M. Tüchler, "Turbo equalisation," *IEEE Signal Processing Mag.*, vol. 21, no. 1, pp. 67–80, Jan. 2003.

[6] X. Wang and H. V. Poor, "Iterative (turbo) soft interference cancellation and decoding for coded CDMA," *IEEE Trans. Commun.*, vol. 47, no. 7, pp. 1046–1061, July 1999.

[7] H. V. Poor, "Iterative multiuser detection," *IEEE Signal Processing Mag.*, vol. 21, no. 1, pp. 81–88, Jan. 2004.

[8] D. Falconer, S. Ariyavisitakul, A. Benyamin-Seeyar, and B. Eidson, "Frequency domain equalization for single-carrier broadband wireless systems," *IEEE Commun. Mag.*, vol. 40, no. 4, pp. 58–66, April 2002.

[9] Z. Wang, X. Ma, and G. B. Giannakis, "Ofdm or single-carrier block transmission," *IEEE Trans. Commun.*, vol. 52, no. 3, pp. 380–394, Mar. 2004.

[10] S. H. Han and J. H. Lee, "An overview of peak-to-average power ratio reduction techniques for multicarrier transmission," *IEEE Trans. Wireless Commun.*, vol. 12, no. 2, pp. 56–65, 2005.

[11] T. Abe and T. Matsumoto, "Space-time turbo equalization in frequency-selective MIMO channels," *IEEE Trans. Veh. Technol.*, vol. 52, no. 3, pp. 469–475, May 2003.

[12] N. R. Veselinović, T. Matsumoto, and M. Juntti, "Iterative STTrC-coded multiuser detection and equalization with unknown inteference," *EURASIP J. Wireless Commun. and Networking*, vol. 2, pp. 309–321, Dec. 2004.

[13] S. Grant and J. Cavers, "Performance enchancement through joint detection of cochannel signals using diversity arrays," *IEEE Trans. Commun.*, vol. 46, no. 8, pp. 1038–1049, Aug. 1998.

[14] T. Walzman and M. Schwartz, "Automatic equalization using the discrete frequency domain," *IEEE Trans. Inf. Theory*, vol. 19, no. 1, pp. 59–60, Jan. 1973.

[15] H. Sari, G. Karam, and I. Jeanclaude, "Frequency domain equalization of mobile radio and terrestrial broadcast channels," in *Proc. IEEE Global Telecommun. Conf. (GLOBECOM) 1994*, pp. 1–5.

[16] M. Tüchler, R. Koetter, and A. C. Singer, "Turbo equalisation: Principles and new results," *IEEE Trans. Commun.*, vol. 50, no. 5, pp. 754–767, May 2002.

[17] K. Kansanen and T. Matsumoto, "A computationally efficient MIMO turbo-equaliser," in *Proc. IEEE Veh. Technol. Conf. (VTC)*, vol. 1, Apr. 2003, pp. 277–281.

[18] C. Laot, R. L. Bidan, and D. Leroux, "Low-complexity MMSE turbo equalization: A possible solution for EDGE," *IEEE Trans. Wireless Commun.*, vol. 4, no. 3, pp. 965–974, May 2005.

[19] M. Tüchler and J. Hagenauer, "Linear time and frequency domain turbo equalisation," in *Proc. IEEE Veh. Technol. Conf. (VTC)*, vol. 4, Oct 2001, pp. 2773–2777.

[20] M. Yee, M. Sandell, and Y. Sun, "Comparison study of single-carrier and multi-carrier modulation using iterative based receiver for MIMO system," in *Proc. IEEE Veh. Technol. Conf. (VTC)*, vol. 3, May 2004, pp. 1275–1279.

[21] P. Schniter and H. Liu, "Iterative frequency-domain equalization for single-carrier systems in doubly-dispersive channels," in *Proc. Annual Asilomar Conf. Signals, Syst., Comp.*, vol. 1, Nov. 2004, pp. 667–671.

[22] J. Karjalainen, K. Kansanen, N. Veselinović, and T. Matsumoto, "Frequency domain joint-over-antenna MIMO turbo equalization," in *Proc. Annual Asilomar Conf. Signals, Syst., Comp.*, Oct. 2005.

[23] J. Karjalainen, N. Veselinović, K. Kansanen, and T. Matsumoto, "Iterative frequency domain joint-over-antenna receiver for multiuser MIMO," in *Proc. Int. Symb. on Turbo Codes*, Apr. 2006.

[24] P. W. Wolniansky, G. J. Foschini, G. D. Golden, and R. A. Valenzuela, "V-BLAST: An architecture for realizing very high data rates over the rich-scattering wireless channel," in *Proc. International Symposium on Signals, Systems, and Electronics (ISSSE)*, Sept. 1998, pp. 295–300.

[25] A. Stefanov and T. Duman, "Turbo-coded modulation for systems with transmit and receive antenna diversity over block fading channels: System model, decoding approaches, and practical considerations," *IEEE J. Sel. Areas Commun.*, vol. 19, no. 5, pp. 958–968, May 2001.

[26] P. Davis, *Circulant Matrices*, 2nd ed. New York: Chelsea Publishing, 1994.

[27] T. Kailath and A. Sayed, *Fast Reliable Algorithms for Matrices with Structure*. Philadelphia: SIAM, 1999.

[28] H. V. Poor and S. Verdú, "Probability of error in MMSE multiuser detection," *IEEE Trans. Inf. Theory*, vol. 43, no. 3, pp. 858–871, May 1997.

[29] P. Robertson, E. Villebrun, and P. Hoeher, "A comparison of optimal and sub-optimal MAP decoding algorithms operating in the log domain," in *Proc. IEEE Int. Conf. Commun. (ICC) 1995*, vol. 2, pp. 1009–1013.

[30] D. Waters, "Complexity analysis of MIMO detectors, http://users.ece.gatech.edu/ deric/projects/mimo/," 2003.

[31] M. Sellathurai and S. Haykin, "TURBO-BLAST: Performance evaluations in correlated rayleigh-fading environment," *IEEE J. Sel. Areas Commun.*, vol. 21, no. 3, pp. 340–349, Apr. 2003.

[32] J. P. Kermoal, L. Schumacher, K. Pedersen, P. E. Mogensen, and F. Frederiksen, "A stochastic MIMO radio channel model with experimental validation," *IEEE J. Sel. Areas Commun.*, vol. 20, no. 6, pp. 1211–1226, Aug. 2002.

[33] H. Oomori, T. Asai, and T. Matsumoto, "A matched filter approximation for SC/MMSE turbo equalisers," *IEEE Commun. Lett.*, vol. 5, no. 7, pp. 310–312, July 2001.

[34] K. Yen and L. Hanzo, "Genetic-algorithm-assisted multiuser detection in asynchronous CDMA communications," *IEEE Trans. Veh. Technol.*, vol. 53, no. 5, pp. 1413–1422, Sept. 2004.

[35] G. Gritsch, H. Wienricher, and M. Rupp, "A union bound of the bit error ratio for data transmission for data transmission over correlated wireless MIMO channels," in *Proc. IEEE Int. Conf. Acoust., Speech, Signal Processing (ICASSP)*, May 2004, pp. 17–24.

[36] 3rd Generation Partnership Project (3GPP); Technical Specification Group Radio Access Network, "Multiplexing and channel coding (FDD) (3G TS 25.212 version 3.2.0 (release 1999))," 3rd Generation Partnership Project (3GPP), Tech. Rep., 2000.

Juha Karjalainen (S'04) received his M.Sc (Tech.) degree in electrical engineering from University of Oulu, Finland, 2001. During 1998-2003 he was with Nokia Mobile Phones, Finland, working as Senior Designer. In 2003, he joined the Centre for Wireless Communications (CWC) where he is currently working towards the Dr. Tech degree. His current research interests include multiuser MIMO communications and iterative equalization techniques.

Nenad Veselinović (S'99, M'05) was born in Serbia in 1975. He received his M.S. and Dr.Sc.(Tech) degrees from University of Belgrade, Serbia in 1999 and University of Oulu, Finland in 2004, respectively. During 2000-2005 he was with the Centre for Wireless Communications, University of Oulu, Finland where he has worked on various projects as a Research Scientist and Project Manager. Since January 2006 he is with Elektrobit, Finland, working as a Senior Specialist and team leader. He has authored and co-authored more than 20 papers in international conferences and journals. His research interests are in general areas of transceiver and protocol design and optimization for wireless communications systems. He is a member of IEEE.

Kimmo Kansanen received his M.Sc (EE) and Dr. Tech. degrees from University of Oulu, Finland in 1998 and 2005, respectively. During and after post-graduate studies he was a research scientist and project manager at the Centre for Wireless Communications at University of Oulu taking part in a number of national and international research projects. On August 2006 he joined the Norwegian University of Science and Technology as a post-doc. His current research interests include multiuser access and scheduling methods, resource allocation, collaborative communications and source-channel coding in wireless systems.

Tad Matsumoto (S'84, SM'95) received his B.S., M.S., and Ph.D. degrees in electrical engineering from Keio University, Yokohama-shi, Japan, in 1978, 1980 and 1991, respectively. He joined Nippon Telegraph and Telephone Corporation (NTT) in April 1980. From 1980 until 1992, he was with Nippon Telegraph and Telephone (NTT), and from 1992 until 1994, he was with NTT DoCoMo, in both of which he experienced a lot of research and development projects. In July 1994 he moved to NTT America, where he served as a senior technical advisor of a joint project between NTT and NEXTEL Communications. In April 1996, he returned to NTT DoCoMo, where, until August 2001, he served as a head of radio signal processing laboratory. In March 2002, he moved to University of Oulu, Finland, where served as a professor at Center for Wireless Communications. Since then he has been very active in research on Turbo equalization techniques for MIMO single carrier broadband mobile communication systems, including algorithm development and complexity reduction, code design and link adaptation, and information theoretic analyses. In 2005, he was appointed a visiting professor, funded by MERCATOR visiting professorship program in Germany. In February 2007, he returned to University of Oulu. Since April 2007, he has been serving as a professor at Japan Advanced Science and Technology (JAIST), while also keeping his part-time professorship at University of Oulu, Finland.

He received IEEE Vehicular Technology Society Outstanding Service Award in 2001, Nokia Foundation Visiting Fellow Scholarship Award in 2002, IEEE Japan Council Award for Meritorious Contributions to Chapter Activities in 2006, IEEE Vehicular Technology Society James R. Evans Avant Garde Award in 2006, and Thuringen State Scientific Award on Advanced Applied Research, Germany, in 2007.

He served as a board-of-governor of the IEEE VT Society for the term from Jan 2002 until Dec 2004, and presently is serving for his second term of the board, from January 2005 until Dec 2007.